Gradus Vol 11, No 1 (2024)
ISSN 2064-8014

PERFORMANCE COMPARISON OF U-TUBE AND COAXIAL BOREHOLE HEAT EXCHANGERS WITH NUMERICAL SIMULATIONS

Mátyás Krisztián Baracza[0000-0002-7809-9069 1*], *József Pap*[0000-0001-9259-0359 1]

[1] Research Institute of Applied Earth Sciences, University of Miskolc, Hungary
https://doi.org/10.47833/2024.1.ENG.006

Keywords:
Geothermal Energy
Heat Production
Borehole Heat Exchanger
Numerical Simulation
Optimization

Article Info:
Received 14. October 2022.
Revised 10. April 2024.
Approved 20. April 2024.

Abstract
It is well known that geothermal heat is a virtually unlimited energy source beneath the ground, which is formed by the radioactive decay of naturally unstable elements. However geothermal energy has been utilized since the ancient ages, it is still a mission for humanity – even in the times of energy crisis with high prices – to find sustainable solutions for high-efficiency heat energy production. Apart from the conventional hydrothermal wells and production/injection systems, an increasing attention is drawn into deep coaxial heat exchangers and heat pumps, utilized in a single wellbore. Optimization of these systems need to be done with an increased care, however it is possible with results obtained from a set of numerical simulations. The present paper investigates hypothetical, single deep "U", "double-U" and coaxial arrangements under different flow rates, where the main target was to analyze efficiency of each model, with short time thermal response simulations.

1. Introduction

The operation principle of any borehole heat exchanger (BHE) is based on the cold working fluid circulated into deeper regions with hot rock media, draining a portion of heat and returning to surface with increased enthalpy. However, an efficient heat pump system consists of many shallow boreholes, gathering heat from deeper areas from a single borehole could result in the same energy outcome, making energy utilization from deep dry hydrocarbon wells a hot topic these days. A promising solution, according to several study is to retrofit these abandoned wells into a coaxial heat exchanger with reverse circulation, which allows working fluid to flow down in the annular side on a lower velocity, draining heat from greater contact area of the casing [1][2][3]. Since energy prices are increasing, a critical design step of such systems is to accurately predict heat performance.

2. Numerical Model

Simulations were carried out with *FlexPDE*, a finite element software from *PDE Solutions Inc* [4]. Model scripts with "U", "double-U" and coaxial arrangements were created with conventional and insulation enhanced setups. To initialize model mesh and mesh multiphysical properties, all sub-geometry dimensions and their relevant thermophysical properties must be set in the script. The following table introduces these values, which served as the final input for 500 m deep models with a single lithology domain, where the domain was extended vertically by an additional 50 m, to provide sufficient heat flow at the bottom section:

* Contact author: Mátyás Krisztián Baracza, E-mail: gfkrixi@uni-miskolc.hu

Table 1.: *BHE sub geometry data with their thermodynamic properties*

SUB GEOMETRY	*R [m]*	*Z [m]*	*k [W/mK]*	*Cp [J/kgK]*	*Density [kg/m3]*
Lithology	20	550	1,79	960	2100
Casing	0,089	500	54	490	7850
Coax-tubing	0,035	500	54	490	7850
U-tube	0,0225	500	54	490	7850
Insulation (optional)	VAR	500	0,05	125	50
Fluid (inner/outer)	VAR	500	0,6	4200	1000

An equation system was set for each scenario. For mass conservation (countercurrent flow of fluid columns), continuity equation was implemented into the script, coupled to the absolute value of velocity vectors:

$$A_1(-V_o) + A_2 v_i = 0 \tag{1}$$

A_1 and A_2 is equal in all “U”-models. For coaxial arrangements, having a static flow rate and uniform cross-section through the pipe gives countercurrent velocities from the following formulae:

$$V_i = \frac{Q}{3600} IR_{tbg}^2 \pi \left[\frac{m}{s}\right] \tag{2}$$

$$V_o = -V_i \frac{IR_{tbg}^2}{IR_{csg}^2 - OR_{tbg}^2} \tag{3}$$

where IR_{csg} is the casing inner radius, OR_{tbg} and IR_{tbg} are tubing radii. Adding insulation of the base models do not affect cross section in “U”-models but reduces annular flow area in coaxial arrangements. In those cases, modification of eq. (2) and eq. (3) was needed.

“U” and “double-U” models were built in Cartesian coordinates, however for reducing total mesh nodes thus reducing total calculation time, it is possible to build all coaxial models in cylindrical coordinates, raising the need for energy equation modification. The following relationship must be valid for each control volume of the model:

$$E_{in} - E_{out} + E_{gen} = E_{steady} \tag{4}$$

With heat in control volume (dx, dy and dz):

$$qx - q(x + dx) + qy - q(y - dy) + qz - q(z + dz) + E_{gen} = E_{steady} \tag{5}$$

If we append the formula with heat flowing though the control volume, and divide resulting equation with dxdydz, we get the following formula for dx,dy,dz → 0:

$$\frac{q"x}{\partial x}\frac{q"y}{\partial y}\frac{q"z}{\partial z} + q = \rho Cp \frac{\partial T}{\partial t} \tag{6}$$

One requirement for experiencing heat flow is the application of Fourier’s law, added to eq. (6) with k tensor derived to x,y and z directions:

$$q"x = -k\frac{\partial T}{\partial x};\ q"y = -k\frac{\partial T}{\partial y};\ q"z = -k\frac{\partial T}{\partial z} \tag{7}$$

then we get a general cartesian heat equation:

$$\frac{\partial}{\partial x}\left(k\frac{\partial T}{\partial x}\right)+\frac{\partial}{\partial y}\left(k\frac{\partial T}{\partial y}\right)+\frac{\partial}{\partial z}\left(k\frac{\partial T}{\partial z}\right)+q=\rho Cp\frac{\partial T}{\partial t} \quad (8)$$

Out model do not have any internal heat source, so q is neglected. On the other hand, flowing fluid raises unstable temperature conditions (where $q \neq 0$) so a convective coefficient was added to the right side of the formula:

$$\frac{\partial}{\partial x}\left(k\frac{\partial T}{\partial x}\right)+\frac{\partial}{\partial y}\left(k\frac{\partial T}{\partial y}\right)+\frac{\partial}{\partial z}\left(k\frac{\partial T}{\partial z}\right)+q=\rho C_p\frac{\partial T}{\partial t}+\rho_f Cp_f V_z\frac{\partial T}{\partial z} \quad (9)$$

Eq. (9) is valid under cartesian coordinates. For cylindrical models, eq. (10) was used:

$$\frac{1}{r}\frac{\partial}{\partial r}\left(kr\frac{\partial T}{\partial r}\right)+\frac{\partial}{\partial z}\left(k\frac{\partial T}{\partial z}\right)+q=\rho C_p\frac{\partial T}{\partial t}+\rho_f Cp_f V_z\frac{\partial T}{\partial z} \quad (10)$$

It is already proven in several studies, that BHE models under normal operating conditions result thermal distance effects not larger than 50 m, however it is always suggested to perform a series of sensitivity simulations to determine safe model boundaries [5][6]. For deeper models, it results a slender cylinder or a slender numerical mesh plane, which often greatly increases total simulation time. In order to eliminate that, we introduced a vertical scaling factor Z_{scale} in the equation, which was coupled with the geometry builder:

$$\frac{\partial}{\partial x}\left(\frac{k\frac{\partial T}{\partial x}}{Z_{scale}}\right)+\frac{\partial}{\partial y}\left(\frac{k\frac{\partial T}{\partial y}}{Z_{scale}}\right)+\frac{\partial}{\partial z}\left(k\frac{\partial T}{\partial z}Z_{scale}\right)+q=\rho C_p\frac{\partial T}{\partial t}+\rho_f Cp_f V_z\frac{\partial T}{\partial z} \quad (11)$$

Geometry initialization needs thermal distribution to be defined. In our models, we assumed a simple, gradually increasing temperature, with T_{grad}=0.045 °C/km, and we initialized thermal distribution based on the following expression:

$$T(z)=T_{surface}+\frac{zT_{grad}}{Z_{scale}} \quad (12)$$

Additional boundary conditions for heat generation at cylinder wall is added into the model, which prevents extensive heat loss from the model. To determine safe boundary as mentioned above, a sensitivity simulation set was carried out, which indicated that short time simulations with 86400 s (1 day) did not obseve changes in soil heat further than 10 m from the wellbore. However to add some safety margin, as seen in *Table 1*, model boundary was set to 20 m.

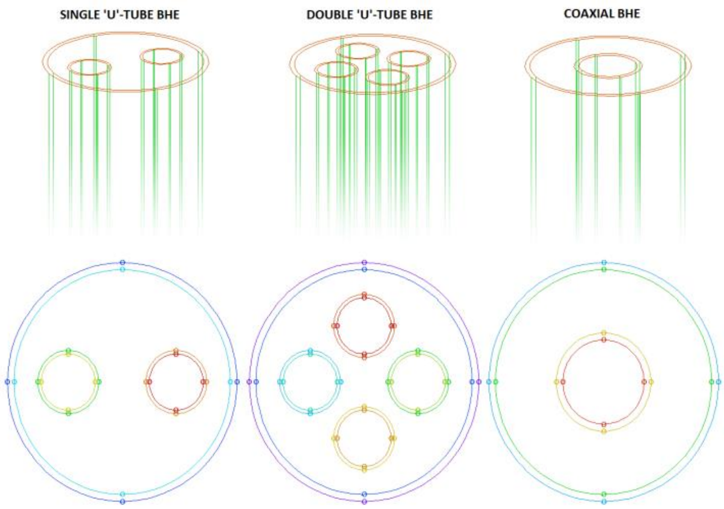

***Figure 1**.: Borehole wireframe of each arrangement*

Surface soil temperature was set to 12°C. Each inlet node was set to fixed temperature at surface (12°C), with $-V_o$ velocities. Each inlet fluid column was averaged at bottom, where resulted average bottomhole temperatures were continuously monitored and forced to be an input value on bottom outlet fluid cells. Top outlet cells were also monitored, wherefrom well performance was calculated.

Produced heat was calculated from the following formula:

$$Q = m * Cp_f * dT \tag{13}$$

where m was determined from the flow rate, and dT from the difference between surface outlet cell temperature and injection temperature.

Well performance was expected to peak shortly after initial well fluid reached surface, then slowly decreasing, close to an equilibrium. To predict performance, total produced heat was also continuously recorded, and then interpolated between each time step.

3. Results

Each simulation was performed with 5 m^3/h and 10 m^3/h flow rates and all 12 PDE script was loaded into a *Python* program for data assessment. Results of each run were labeled, and then imported to an excel workbook, with visual outputs for each time step. From the output visual itself, it was clear that the effect of insulation has a significant effect to the output, as seen on the figure below:

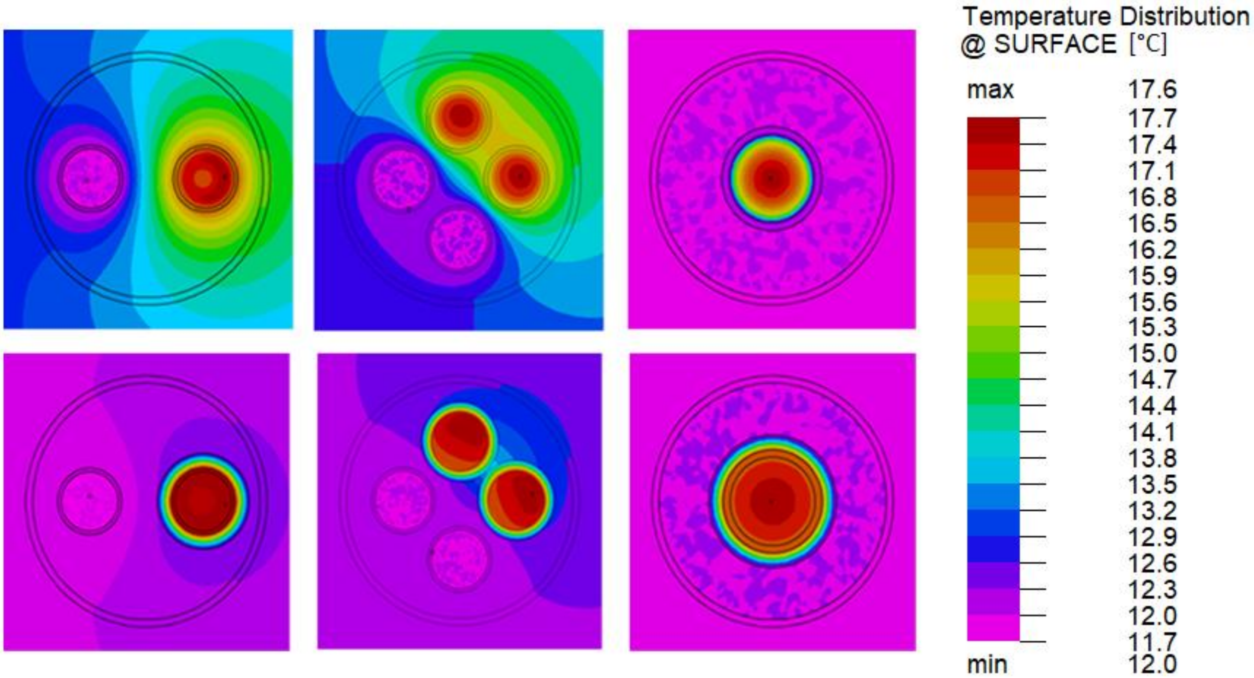

***Figure 2.**: Visual results: Surface temperature distribution around the wellbore for "U"-tube profile [left], "double-U"-tube profile [middle] and coaxial well [right]. Images in the bottom row represent insulated structures, where heat dissipation to the formation is greatly reduced (t=1 day, Q=5 m^3/h)*

Temperature averages on bottom and surface were recorded for each simulation, then we calculated heat performance for each case. From the result dataset and simulation metafiles, we observed the following:

- Coaxial arrangements have slightly better performance in shallow environment for short-time continuous operation
- Single / double-U systems have their returning fluid column heated up at the bottom section, causing wellhead temperature to be higher than bottom-hole (as illustrated on *Fig. 3.*).
- Heat link between fluid columns at coaxial BHE increases bottom fluid temperature while dampens bottom heat drainage, thus wellhead temperature is slightly higher compared to other arrangements
- Insulated systems initially showed a peak in produced heat but they have no performance enhancement effect for extended operations
- Increasing flow rate from 5 m^3/h to 10 m^3/h slightly increases short time performance while sustainability greatly reduces.

The following table summarizes obtained bottom hole and wellhead temperatures in addition with each calculated end time performance value:

***Table 2.**: Result obtained from each simulation (t=1 day)*

BHE ARRANGEMENT	*FLOW RATE: 5 m³/h*			*FLOW RATE: 10 m³/h*		
	FLOWLINE TEMP [°C]	*BOTTOM TEMP [°C]*	*P_ENDTIME [kWh]*	*FLOWLINE TEMP [°C]*	*BOTTOM TEMP [°C]*	*P_ENDTIME [kWh]*
SINGLE_U	15.27	14.40	19.21	13.85	13.17	21.62
SINGLE_U_INS	14.91	14.73	17.00	13.56	13.44	18.43
DOUBLE_U	15.45	15.29	20.25	14.00	13.51	23.53
DOUBLE_U_INS	15.31	15.18	19.47	13.79	13.65	21.03
COAXIAL	15.85	18.13	22.50	14.23	15.09	26.22
COAXIAL_INS	16.08	16.47	23.98	14.29	14.42	27.03

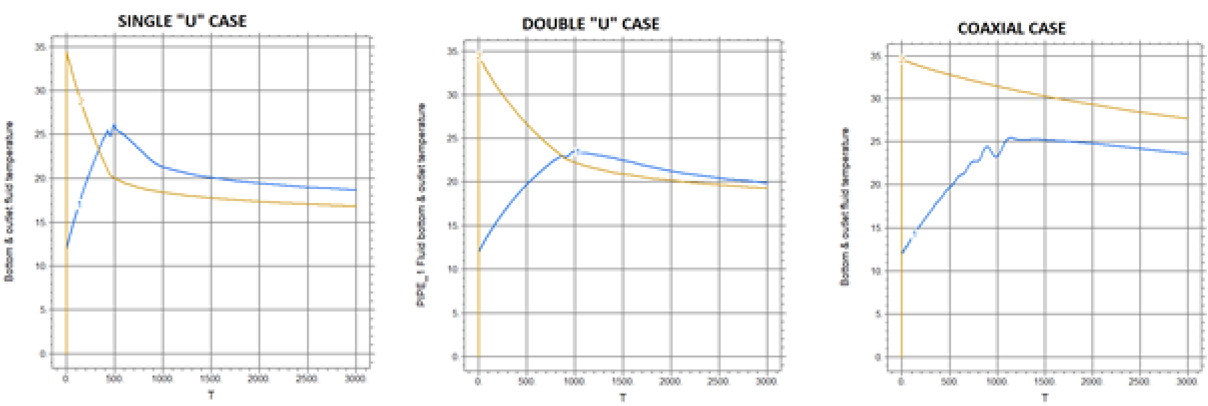

***Figure 3.**: Bottom hole and wellhead average fluid cell temperature (t=3000s, Q=5 m3/h, without insulation)*

Performance optimization of each BHE requires clarification of many operational and design parameters, considering all geological and well structural capabilities:

- injection rate and temperature
- diameter of production tubing (which has a significant role on fluid velocities)
- operation schedule (continuous/intermittent)
- null-point temperature (reinjection)

For retrofitting any abandoned hydrocarbon well, usually deeper regions are reached thus increased wellhead temperature and performance is expected, which means we have to pay attention to every parameter above. We ran additional simulations with the base coaxial model, flow rates between 2,5-27,5 m^3/h, with extending simulation time to 604800 s (1-week continuous operation).

As seen from the results, increased flow rate resulted in a wellhead temperature drop while performance slightly increased. However, deriving performance from an increased null-point value (which means reduced dT) should indicate, that peak well performance is not necessarily found at highest flow rate. *Fig. 4*. represents, that peak well performance dropped from 20.63 kW/h to 11.13 kW/h in a week while it's corresponding flow rate reduced to 5 m^3/h.

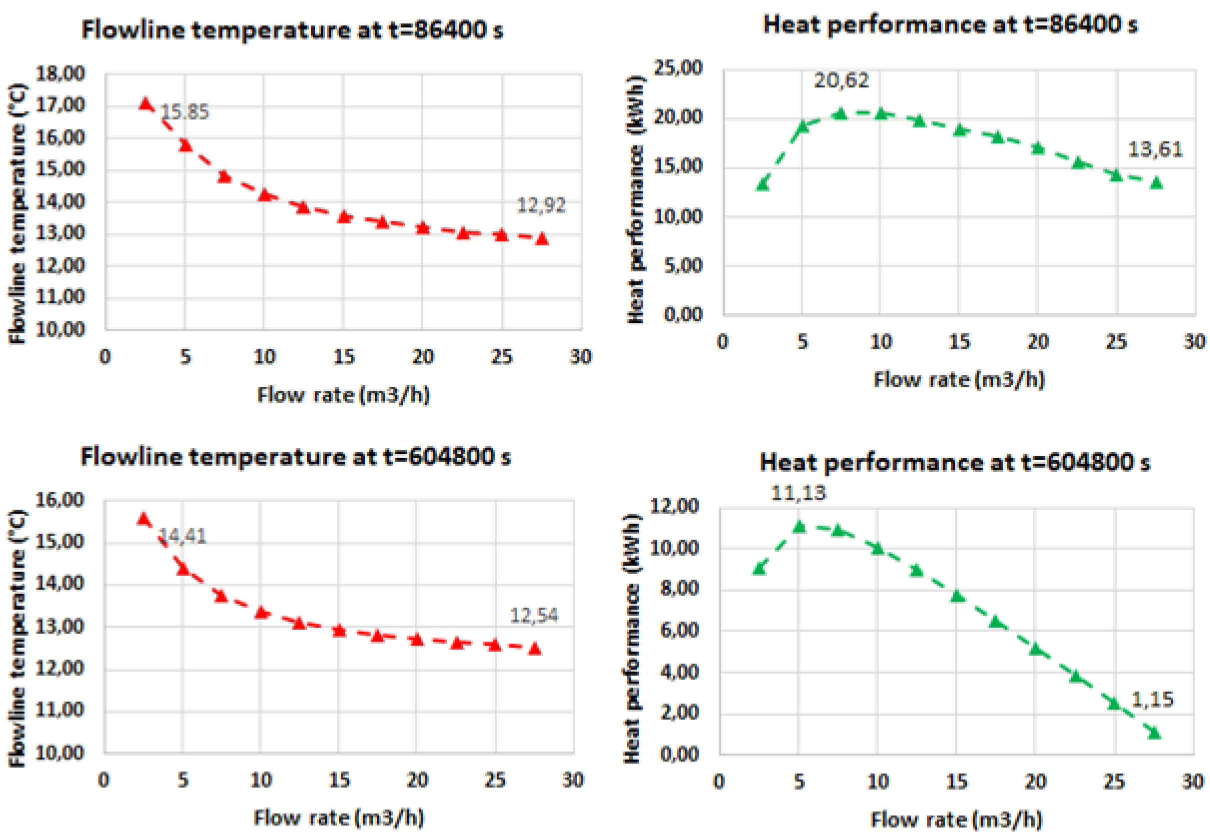

Figure 4.: *Wellhead temperature and performance of coaxial heat exchangers at 1 day continuous operation [top] and 1 week continuous operation [bottom] in function of flow rate*

4. Conclusion

We have successfully designed numeric models built in *FlexPDE* based on *Table 1.*, which was coupled with a *Python* program to run simulations. We concluded that with both 5m^3/h and 10 m^3/h simulation sets, maximum performance was reached with double-U installations. We ran additional simulations with a set of flow rates using the base coaxial model, wherefrom we were able to predict peak performance.

Acknowledgement

The research was carried out in the framework of the GINOP-2.3.2-15-2016- 00010 “Development of enhanced engineering methods with the aim at utilization of subterranean energy resources” project of the Research Institute of Applied Earth Sciences of the University of Miskolc in the framework of the Széchenyi 2020 Plan, funded by the European Union, co-financed by the European Structural and Investment Funds.

References

[1] Aniko N. Toth, Peter Szucs, Jozsef Pap, Attila Nyikos, David K. Fenerty: Converting Abandoned Hungarian Oil and Gas wells into Geothermal Sources - PROCEEDINGS, 43rd Workshop on Geothermal Reservoir Engineering - Stanford University, Stanford, California, SGP-TR-213.

[2] Jasmin Raymond, Serge Mercier, Luc Nguyen: Designing coaxial ground heat exchangers with a thermally enhanced outer pipe – Geothermal Energy – SPRINGER, 2015 (vol. 3), p 1-14. DOI: 10.1186/s40517-015-0027-

[3] Morgan Lee Lous, Francois Larroque, Alain Dupuy, Adeline Moignard: Thermal performance of a deep borehole heat exchanger: Insights from a synthetic coupled heat and flow model - Geothermics, ELSEVIER 2015 (57), p. 157–172. DOI: 10.1016/j.geothermics.2015.06.014

[4] PDE Solutions Inc. - FlexPDE 6: PDE Solutions Inc.; 2011.

[5] Templeton, J.D., Ghoreishi-Madiseh, S.A., Hassani, J.D. and Al-Khawaja M.J.: Abandoned petroleum wells as sustainable sources of geothermal energy, Elseviere, Energy, Volume 70, 1 (2014), 366-373

[6] [Heyi Zeng, Nairen Diao, Zhaohong Fang: Heat transfer analysis of boreholes in vertical ground heat exchangers – International Journal of Heat and Mass Transfer – vol. 46, issue 23, p. 4467-4481. DOI: 10.1016/S0017-9310(03)00270-9

[7] Richard A. Beier: Transient Heat transfer in a U-tube borehole heat exchanger – Applied Thermal Engineering – vol. 62, issue 1, p. 256-266. DOI: 10.1016/j.applthermaleng.2013.09.014